THE JOURNAL OF PHYSICAL CHEMISTRY B

Article

pubs.acs.org/JPCB

Structural Water Cluster As a Possible Proton Acceptor in the Adduct Decay Reaction of Oat Phototropin 1 LOV2 Domain

Ruby H. Chan and Roberto A. Bogomolni*

Department of Chemistry and Biochemistry, University of California, Santa Cruz, California 95064, United States

ABSTRACT: LOV domains (Light, Oxygen, Voltage) are the light-sensory modules of phototropins, the blue-light photoreceptor kinases in plants, and of a wide variety of flavoproteins found in all three domains of life. These 12 kDa modules bind a flavin chromophore (FMN or FAD) noncovalently and undergo a photochemical activation in which the sulfur atom of a conserved cysteine forms an adduct to the C(4a) carbon of the flavin. The adduct breaks spontaneously in a base-catalyzed reaction involving a rate-limiting proton-transfer step, regenerating the dark state in seconds. This photocycle involves chromophore and protein structural changes that activate the C-terminal serine/threonine kinase. Previous studies (*Biochemistry* **2007**, *46*, 7016−7021) showed that decreased hydration obtained at high glycerol concentrations stabilizes the adduct state in a manner similar to that attained at low temperatures, resulting in much longer adduct decay times. This kinetic effect was attributed to an increased protein rigidity that hindered structural fluctuations necessary for the decay reaction. In this work, we studied the adduct decay kinetics of oat phototropin 1 (phot1) LOV2 at varying hydration using a specially designed chamber that allowed for measurement of UV−visible and FTIR spectra of the same samples. Therefore, we obtained LOV protein concentrations, adduct decay kinetics, and the different populations of bound water by deconvolution of the broad water absorption peak around 3500 cm^{-1}. A linear dependence of the adduct decay rate constant on the concentration of double and triple hydrogen-bonded waters strongly suggests that the adduct decay is a pseudo-first-order reaction in which both the adduct and the strongly bound waters are reactants. We suggest that a cluster of strongly bound water functions as the proton acceptor in the rate-limiting step of adduct decay.

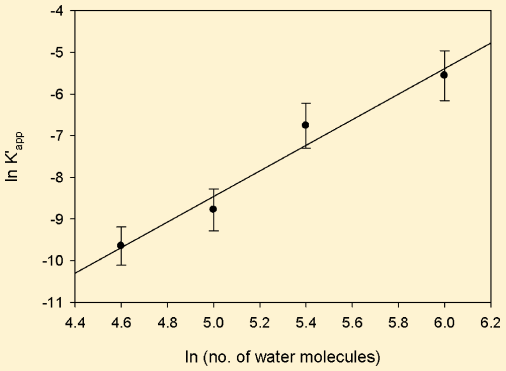

I. INTRODUCTION

Phototropins[1,2] are a class of blue-light receptors that are involved in phototropic plant movement,[1−4] chloroplast relocation,[5,6] and stomatal opening in guard cells.[7] Two plant phototropins (phot1 and phot2)[1] and the fern *Adiantum capillus-veneris* and *Chlamydomonas reinhardtii*[8] homologues are ∼120 kD proteins that contain a C-terminus serine/threonine kinase and two light-sensing domains, the LOV domains, within their N-terminal segments. The LOV (Light, Oxygen, Voltage) domains belong to the super family of PAS (Per/Arnt/Sim) domains.[9] Both C- and N-terminus domains with a variety of predicted functions are present within LOV domain proteins.[10,11] It has been shown for some and predicted for others that these domains serve as the output-signaling component of the LOV light sensors. These output domain (C or N) components function as enzymes (kinases, phosphodiesterases), gene expression regulators, circadian control, and transcriptional regulators.[11,12] Often the LOV protein has been isolated, but only a few physiological functions have been identified, and no signal transduction mechanism has been fully elucidated yet. Among the few that have been studied are the sensory histidine kinases of the soil bacterium *Caulobacter cressentum*,[13] the animal pathogens *Brucella mellitensis* and *Brucella abortus*,[14] the LOV-STAS domain (sulfate transporters anti-sigma factor antagonist) protein (YtvA) of the soil bacterium *B. subtilis*,[15] which was shown to be involved in blue-light regulation of the bacterium general stress response, the LOV domain of FKF1 (an *Arabidopsis* LOV protein), which is known to form dimers with Gigantea and Constans in a blue-light dependent manner,[16,17] and VVD, a small LOV domain protein that undergoes a large-scale conformation change from homo- and heterodimers with WC-1 to regulate circadian gene transcription in *Neurospora crassa*.[18]

LOV domains undergo a photochemical activation in which the sulfur atom of a conserved cysteine forms in microseconds an adduct to the C(4a) carbon of the flavin. The adduct breaks spontaneously in a base-catalyzed reaction,[19] involving a rate-limiting proton (or hydrogen atom) transfer step,[20,21] regenerating the dark state in times ranging from seconds in phototropin's LOV domains to minutes and hours in bacterial and fungal LOV domain proteins.[14,21,22] This photocycle involves chromophore and protein structural changes that propagate to the rest of the molecule-activating enzymatic activities, for example, serine/threonine kinase in phototropins[2] and bacterial sensory histidine kinases[13,14] and phosphodies-

Special Issue: B: Richard A. Mathies Festschrift

Received: May 21, 2012
Revised: July 9, 2012
Published: July 30, 2012

   dx.doi.org/10.1021/jp304934t | *J. Phys. Chem. B* 2012, 116, 10609−10616

terases.[23] The photocycle of oat phototropin 1 (phot1) LOV2 involves the formation in a few nanoseconds of an FMN triplet state that absorbs in the 650 nm range.[24] About 50% of this triplet state relaxes back to the ground state and ~50% forms the intramolecular FMN-cysteine adduct,[21] which has been identified as the signaling intermediate state of this photoreceptor. Both the adduct formation and decay mechanisms involve rate-limiting proton transfer, and the decay is base-catalyzed.[19,20,25] Of particular interest is the identification of the proton acceptor group (the catalytic base) in the adduct decay reaction. Available crystal structures of the LOV2 domains from the fern *Adiantum* phy3 phototropin[26] and from the LOV1 domain of the phototropin from the unicellular algae *Chlamydomonas reinhardtii*[27] show that no basic amino acid residues are close enough to serve as the base catalyst in either molecule. Both structures contain two or more conserved structural water molecules, one of which is in direct hydrogen-bonding interaction with the FMN chromophore. This water is part of a solvent channel that has been suggested to be involved in a H-bonding relay that functions as the catalytic base.[25,28] In addition, both adduct formation[29] and decay reactions have been shown to involve perturbation of water molecules.[30,31] The presence of a glutamine residue in hydrogen-bonding interaction with the FMN seems to have an important role in the kinetics of the photocycle of the LOV domain of EL222, a DNA binding domain protein from marine bacterium *Erythrobacter litoralis* HTCC2594[32] and in LOV2 of *Adiantum* Phytochrome3.[33] It should be noted that models have been previously advanced, invoking proton relay via structural waters or hydrogen-bonded networks from the flavin N5−H to specific protein side chains or even directly to the thiolate.[25,28] However, the putative catalytic base has not yet been experimentally identified.

FTIR spectra have shown hydrogen-bonding perturbations of water molecules during adduct formation,[29] and our group reported that the adduct decay is blocked at low hydration level.[30] Iwata et al.[31] using glycerol as the dehydrating agent, confirmed this early observation. This group reported a hydration dependence of the adduct decay kinetics and of protein structural changes of *Adiantum* phy3 LOV2 during the decay reaction. These authors also showed that the effect of dehydration on the kinetics was similar to the effect of lowering the temperature.[31] The data were interpreted as an effect of dehydration on protein structural rigidity. These authors attempted to quantify the number of water molecules per protein molecule at different dehydration levels using the water infrared stretching vibration bands at ~3500 cm^{-1} and the protein amide vibrations. Even at the lowest hydration levels reached, the water content was on the order of 10^3 or higher per LOV2 molecule. These large values prompted the conclusion that the decrease in bulk (or surface hydration) water was controlling the reaction rate by affecting protein structural fluctuations.

A qualitative observation in our previous work was that as dehydration proceeds, the maximum in the infrared absorption of water shows a gradual shift to lower wave numbers, consistent with the removal of water molecules having different degrees of hydrogen bonding. As the number of hydrogen bonds increases, the OH vibration stretching frequencies shift to a lower wavenumber.[34,35]

We hypothesized that the different water subpopulations could have different roles in the photochemistry and that perhaps the most firmly bound (structural) waters could serve as proton acceptors in the decay reaction or serve as a bridge for the transport of the proton to a remote base. This prompted us to correlate quantitatively the concentration of the different water populations, at progressively higher dehydration levels, with the adduct decay kinetics. This required measuring both the UV−visible absorption spectrum and the infrared spectrum of the water stretching in the same sample and under identical conditions of dehydration. Using known extinction coefficients for FMN in the visible spectrum and for the water absorption peaks in the infrared, we evaluated the molar ratio of water/FMN and consequently the water/LOV2 protein ratio. A simple inspection of the published spectra by Iwata et al. and of our unpublished preliminary results indicates that the very broad water absorption band in the IR contains several bands at different frequencies, which should correspond to the well-known hydrogen-bonded water subpopulations.[34,35]

In this work, we designed and constructed a special chamber that allows the control of the hydration level of the oat LOV2 films by equilibrating with saturated solutions of different salts placed in a special compartment connected to the sample film through gaseous exchange. This approach has been used successfully in numerous previous studies.[36,37] Analysis of the broad water absorption in terms of the contribution of those subpopulations allowed us to establish the correlations between each individual population and the adduct decay kinetics. We report here that a subpopulation of strongly bound water molecules, presumably those structurally attached to the flavoprotein, control the rate of adduct decay in a concentration-dependent manner, which suggests that an intramolecular water cluster of strongly hydrogen-bonded water, in the proximity of the chromophore, may function as the primary acceptor in the proton- transfer reaction in the oat phot1 LOV2 adduct decay mechanism.

II. EXPERIMENTAL SECTION

II.1. Sample Preparation and Optical Chamber. The oat phot1 LOV2 protein used in this study contains an N-terminal calmodulin-binding peptide. It was expressed in *E. coli* and purified by a calmodulin affinity column as previously described.[16,30] Salt and buffer in the samples were removed by dialysis against distilled water for 16 h in cold and darkness before lyophilization. The final sample containing 2 mg of protein (calculated from the LOV2 extinction coefficient of 13 800 M^{-1} cm^{-1}) was lyophilized and resuspended in 120 μL of water. For the UV−visible kinetics measurements at different hydration levels, about 20 μL of resuspended sample was placed on quartz windows and allowed to dry under a slow flow of dry nitrogen forming a stable thin film. These supported films were placed in the dehydration chamber (described below) to achieve the final hydration level for the spectroscopic measurements. The spectra were recorded on a Hewlett-Packard 8452A diode array spectrometer with a sample holder specially designed to accommodate the dehydration chamber. For measurements of the UV−vis absorption and FTIR spectra on the same sample, the sample film was formed onto a BaF_2 window (International Crystal Laboratories, Garfield, NJ). The FTIR film samples used to evaluate the number of water molecules per flavoprotein were thinner and therefore less concentrated than those used in our general kinetic studies in the UV−vis range. This was necessary to avoid infrared signal saturation. As a result, the visible spectrum (maximum absorption ~0.01 OD) had a poorer signal-to-noise ratio (approximately 8:1).

We used gaseous equilibration with different saturated salt solutions to control the RH of the sample films. The saturated-salt solution method is well-established and is based on the different vapor pressures of water resulting from the specific solute−solvent interactions present in the different saturated salt solutions. We used saturated solutions of: NaCl (75% RH), $Mg(NO_3)_2$ (53%), $MgCl_2$ (33%), and LiCl (11%).[38]

Because our method of controlling humidity required using a saturated salt solution only in gaseous contact with the sample film, we had to design a special chamber equipped with a solution reservoir (Figure1). The chamber consisted of a

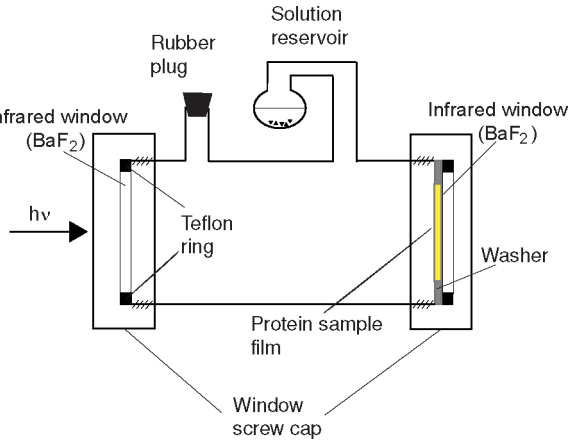

Figure 1. Schematics of the sample chamber (for description, see text).

specially machined horizontal cylindrical Teflon tube (approximately 3 cm in diameter and 7 cm long) closed at each end by removable BaF_2 windows held in place by a screw cap. A Teflon ring was placed between the window and the screw cap to achieve a good seal. The window with dehydrated protein film deposited was placed on the inside surface of the window closer to the instrument detector. A plastic washer acting as a diaphragm was placed between the Teflon ring and the window to restrict the cross section of the measuring beams (both IR and UV−vis) to be fully within the sample area.

The top of the chamber contained two openings. A rubber plug typically closed one opening, and the other supported the saturated salt solution glass reservoir. The solution reservoir was placed on the side closer to the protein sample. The protein samples were allowed to equilibrate to the respective RH overnight in the dark. To achieve even higher dehydration levels, we resorted to sample equilibration using dry nitrogen gas flow. In this case, we simply replaced the solution reservoir with a tube connected to the dry nitrogen flow and left the other opening unplugged to permit the gas flow. For the UV−vis measurements, the nitrogen flow was continued during measurements. For the FTIR work, where the entire measuring sample compartment of the instrument is purged with dry nitrogen, the two openings were left open and the entire sample chamber was allowed to equilibrate inside the FTIR sample compartment overnight in the dark.

II.2. UV−vis and FTIR Spectroscopy. Following photolysis of the oat LOV2, time-resolved optical difference spectra were collected for up to several hours using a Hewlett-Packard 8452A diode array spectrometer driven via a GPIB interface (IEEE 488) and LabVIEW software for automated control of data acquisition (LabVIEW (National Instruments, Austin, TX) as previously described.[14] A continuous broadband excitation beam was provided by a fiber optic illuminator (V-LUX 1000, Volpi Mfg., USA) filtered through a Corning Glass (model 5-56) filter with a maximum transmission at 420 nm and ∼80 nm half-bandwidth. The sample was illuminated for 1 min to reach near-saturation, creating as much of the excited population as possible. The temperature was not controlled but was recorded to be 23.5 ± 0.5 °C.

FTIR spectra were recorded on a Thermo Nicolet 870 spectrometer (Madison, WI) equipped with a liquid-nitrogen-cooled MCT detector. OMNIC software (Version 6.2 Thermo-Nicolet) controlled the FTIR instrument and provided some capabilities for data reduction and analysis. Typically 128 interferograms in the range of 4000−740 cm^{-1} with a spectral resolution of 4 cm^{-1} were recorded and averaged. Automatic instrumental baseline correction was applied using OMNIC, and all spectra were normalized to the intensity of the amide II band at ∼1450 cm^{-1}. We chose this band because the region is not affected by the varying water absorption at ∼1640 cm^{-1} (in-plane bending modes).[39] This normalization was never more than a few percent and yet was necessary because the path length through the films varied slightly at different hydration levels.

II.3. Data Analysis. Data analysis to determine the contribution of the different populations of free and hydrogen-bonded water was carried out in the OH stretching region (2800 to 3800 cm^{-1}). We deconvoluted this broad band into its four main species using the four-component mode, which takes into account the IR bands usually observed for water vibration.[40,41] This model is based on studies of polyprolylene/ethylene alcohol vinyl polymers and assigns peaks at around 3600, 3500, 3400, and 3200 cm^{-1} to free, singly hydrogen-bonded, doubly hydrogen-bonded, and triply hydrogen-bonded water molecules, respectively. Curve fitting was carried out using GRAMS-32 software (Galactic Industries). Component bands were fitted assuming a mixture of Gaussian and Lorentzian line shapes. In one case, at low hydration levels (11%), the water absorption band at 3200 cm^{-1} could not be unambiguously determined because of the overlap with background IR absorption of the sample. We resorted to assume a linear behavior between the 33% and the N_2 dried sample to estimate this value in Table 2.

The same protein film sample was used for UV−vis absolute spectrum and FTIR measurements to calculate the number of water molecules at a specific hydration level. The molar ratio of water molecules per flavoprotein was calculated using molar extinction coefficients of the UV−vis absorption of oat LOV2 (13 800 M^{-1} cm^{-1} at 450 nm)[42] and the infrared absorption of the OH stretch of free water (100 M^{-1} cm^{-1} at 3500 cm^{-1}).[43] The same extinction coefficient was used for the hydrogen-bonded waters. Although theoretical calculations[44] show some variations due to the additional interactions, they are not large, and, more importantly, the absolute values would not affect the main conclusions of our work, namely, that a subpopulation of water molecules controls the reaction rates. Because the protein sample was a film instead of a solution, we had to assume that all molecules in the measuring beam were distributed over the area of the film and use Beer's law with absorption cross sections and the number of molecules per unit area. This is a common procedure for these types of film samples. In brief, Beer's law states that

$$I_t = I_o 10^{-A} \text{ with } A = \varepsilon c l \quad (1)$$

dx.doi.org/10.1021/jp304934t | J. Phys. Chem. B 2012, 116, 10609−10616

where ε is the molar extinction coefficient (M^{-1} cm^{-1}), c is the molar concentration (M), and l is the path length (cm). A is the absorbance and is unitless. An alternate way to express the absorbance of a film sample is: $A = \sigma N$, where σ is the absorption cross section (cm^2/molecule), and N is the number of molecules per cm^2.[45] The extinction coefficient was converted to σ as follows

$$\sigma(\mathrm{cm}^2/\mathrm{molecule}) = \varepsilon(\mathrm{L/mol\cdot cm}) \times (\mathrm{mol}/6 \times 10^{23}\mathrm{molecule}) \times (10^3\ \mathrm{cm}^3/\mathrm{L}) \quad (2)$$

This yields a σ^{FMN} at 450 nm and σ^{water} at 3500 cm^{-1} of 2×10^{-17} cm^2/molecule and 1.7×10^{-19} cm^2/molecule, respectively. Global kinetic analysis of the data yielded first-order decay rates used in this work. Kinetic analysis methods were as previously described.[46]

III. RESULTS AND DISCUSSION

III.1. Photocycle Kinetics at Various Hydration Levels. Figure 2 shows the difference spectra of the adduct recovery at

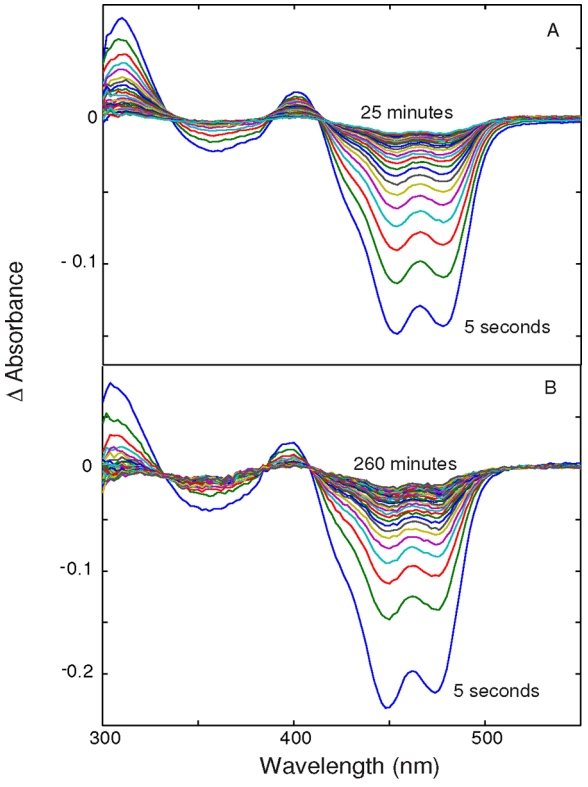

Figure 2. Absorbance changes at 75% hydration (A) and 53% hydration (B). The time indicated above the traces is the last delay time, and the time indicated at the bottom of the traces corresponds to the first delay time.

75 and 53% hydration levels, respectively. Both samples showed photocycle lifetimes much longer than the solution sample, but the sample at 53% hydration was significantly slower than the one at the 75% hydration level. Difference spectra of protein films equilibrated to 33% relative humidity (RH), 11% RH, and house nitrogen were also taken (data not shown); these showed progressively slower adduct decay kinetics. Even the nitrogen-purged sample decayed, albeit in several hours. Instability of the single-beam instrument became significant at these extremely long times, rendering the spectra unfit for a reliable global kinetic analysis.

III.2. Molar Ratio of Bound Water to Protein. Analysis of the FTIR spectra in the water absorption region indicates the presence of the typical protein amide A (the NH_2 stretches) absorption band at ~3200 cm^{-1}, amide B (the NH_2 stretches and bendings) and the absorption from the protein C−H stretch vibrations in the 2900−3000 cm^{-1} range.[47] At high hydration levels, the absorption of free water at 3500−3600 cm^{-1}, is evident, but it gradually disappears at lower hydration levels (Figure 3). To resolve the water absorption into its

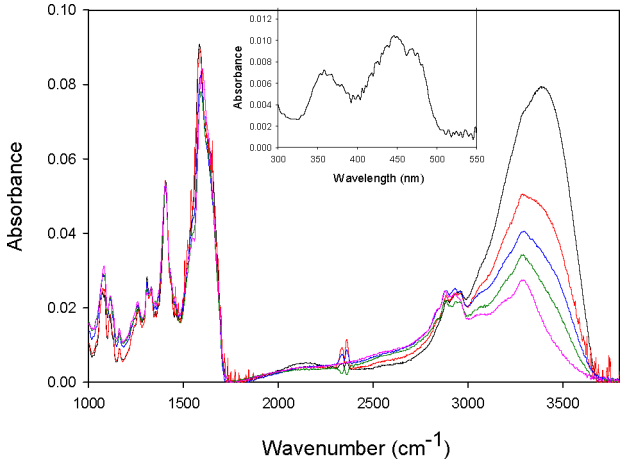

Figure 3. FTIR spectra of the oat phot1 LOV2 film hydrated using NaCl (75% relative humidity (RH); black line), $Mg(NO_3)\cdot 6H_2O$ (53% RH; red line), $MgCl_2\cdot 6H_2O$ (33% RH; blue line), and $LiCl\cdot H_2O$ (11% RH; green line) and dry nitrogen (pink line). All of the spectra were baseline-adjusted and normalized to the spectrum of the dry-nitrogen-equilibrated film on the basis of the amide II stretching band (1450 cm^{-1}). Insert: UV−vis absorption spectrum of the protein sample used for the FTIR experiments.

different sub-populations and to generate spectra containing only the water absorption (pure water spectra), we ideally would want to subtract the protein contribution. As a first approximation, we subtracted the spectrum of the nitrogen-purged sample from all other spectra (Figure 4). Hydration-independent peaks from C−H and NH_2 were removed after subtraction, and the spectral features that remained should be due to water only. Even under dry nitrogen some strongly bound water remained, as shown below in our spectral analysis of the nitrogen-dried sample. Because its spectral contribution has been removed in this procedure, we corrected the final data by adding up this small amount of strongly hydrogen bonded water absorption (see below).

The subtracted spectra of 75, 53, and 33% RH were subjected to spectral deconvolution to obtain components of water FTIR peaks in the region 2800−3800 cm^{-1}, as described by Roge et al.[35] In their results, peaks designated 4, 3, 2, and 1 correspond to free (non-hydrogen-bonded) water, singly hydrogen-bonded water, doubly hydrogen-bonded water, and triply hydrogen-bonded water, with absorption maxima at around 3600, 3500, 3400, and 3200 cm^{-1}, respectively. We will use the same peak numbering system herein.

Figure 5A,B shows the curve-fitting analysis of the adjusted FTIR spectra of at 75 and 33% RH, respectively. A very broad peak at ~3100 cm^{-1} (not shown) was added to accommodate

dx.doi.org/10.1021/jp304934t | J. Phys. Chem. B 2012, 116, 10609−10616

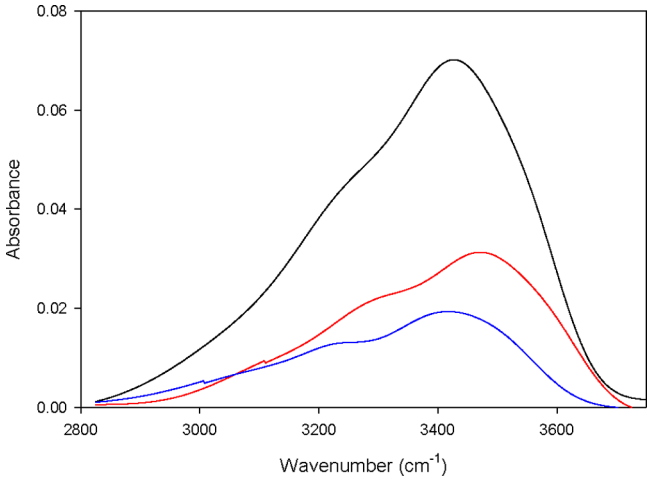

Figure 4. FTIR spectra of the protein-bound water. FTIR spectra of the film at 75% RH (black), 53% RH (red), and 33% RH (blue) after subtraction of the protein contribution. The dry-nitrogen-equilibrated protein spectrum was subtracted from each spectrum to obtain the so-called "pure water" spectra. Methyl stretches around 2900−3000 cm^{-1} and the NH_2 regions around 3200 (amide A) and 3050 cm^{-1} (amide B)[47] were subtracted out.

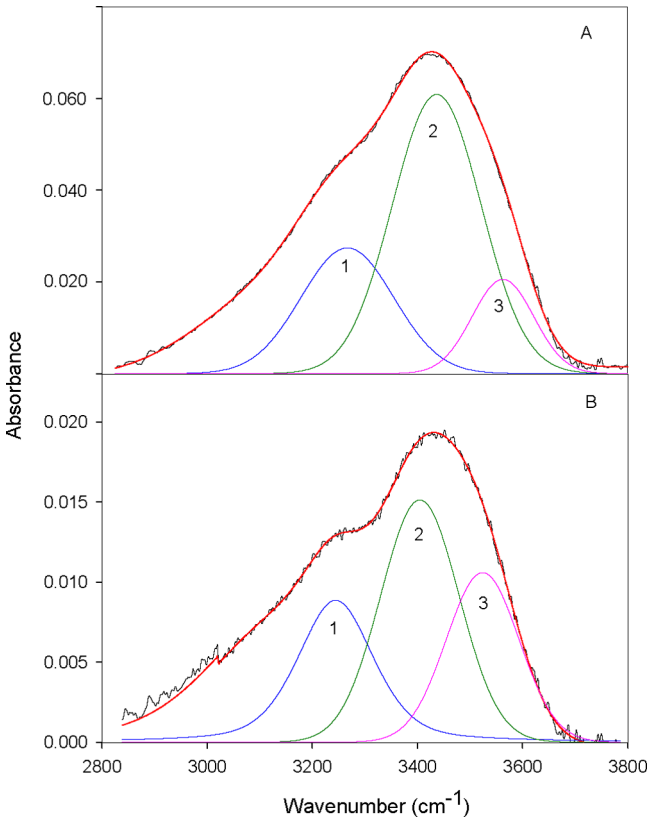

Figure 5. Curve-fitting analysis of the FTIR spectrum corresponding to water molecules at 75 (A), and 33% (B). The Figure displays the experimental line shape (black), curve fit (red), and the four resolved components. Peaks 3 (pink), 2 (green), and 1 (blue) correspond to singly, doubly, and triply hydrogen-bonded water, respectively.

the truncation of the data. We notice that already at 75% RH, peak 4, which represents free water, is no longer present. The deconvolution analysis of the nitrogen-equilibrated sample indicates that both the double and triply hydrogen-bonded water populations are still present (Figure 6). Therefore, by this procedure, we subtracted not only the absorption of the protein

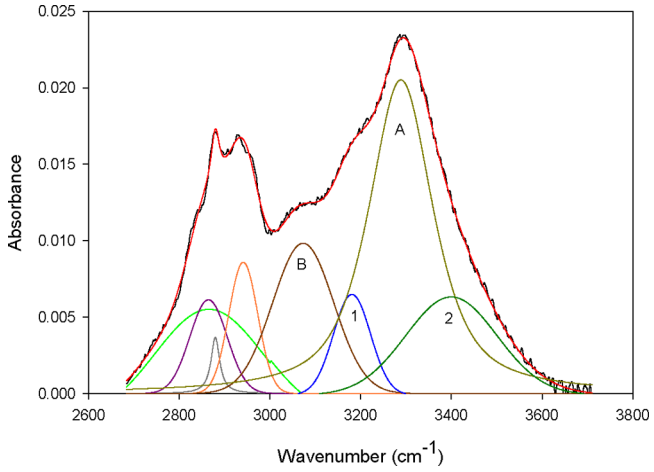

Figure 6. Curve-fitting analysis of the FTIR spectrum of the dry-nitrogen-equilibrated sample. Peaks 3 and 4, which correspond to free and singly hydrogen-bonded water, are completely absent. Only peaks 1 and 2 remain. Peak A is the absorption band of the protein amide A vibration. Peak B at 3050 cm^{-1} corresponds to amide B vibrations. Peaks in the 2900 cm^{-1} are due to the methyl stretches.

but also the contribution of the remaining strongly bound water. This absorption (~0.005 absorbance unit) was added back to the 3200 cm^{-1} peaks of subpopulation in our deconvolution analysis of the "pure water" spectra.

The quality and reproducibility of the fit to the four water subpopulations was excellent. It showed a complete loss of the free water contribution at >3600 cm^{-1}, followed by the gradual removal of the ~3500 and ~3400 cm^{-1} water contributions. At the highest dehydration reached, the main contributions were from the triply hydrogen bound water at 3200 cm^{-1} and double hydrogen-bound water at 3400 cm^{-1}. These two forms seem to be in equilibrium because they decrease together at higher dehydration. Table 1 shows the gradual decrease in the FTIR

Table 1. Summary of the Deconvolution of the FTIR 3500 cm^{-1} Stretch Region at 3100−3500 cm^{-1}[a]

relative humidity (% RH)	$A_{3500cm^{-1}}$ (peak 3)	$A_{3400cm^{-1}}$ (peak 2)	$A_{3200cm^{-1}}$ (peak 1)
75	0.02	0.06	0.027
53	0.01	0.03	0.016
33	0.01	0.015	0.009
dry nitrogen	absent	0.006	0.006

[a]Peak at $A_{3600cm^{-1}}$ is absent.

absorbance of the deconvoluted water peaks. Absorbance at 3200 cm^{-1} was used to calculate the number of strongly bound water molecules per flavoprotein. Photocycle kinetics results and the molar ratios of water per flavoproteins are summarized in Table 2.

Plots of the rate constant of adduct decay as a function of triply H-bonded water molecules present in the samples (or their natural logarithms to better graphically illustrate the large span of rate constant values) yield a straight line (Figure 7). The same holds true when the rate constant is plotted against doubly H-bonded water molecules. A simple model that readily accounts for this result is that the two types of strongly bound

dx.doi.org/10.1021/jp304934t | J. Phys. Chem. B 2012, 116, 10609−10616

Table 2. Summary of the UV−vis Kinetics Data and the Calculation of the Number of Water Molecules Using the Absorbance at 3200 cm^{-1} from the Deconvoluted FTIR Data[a]

relative humidity (% RH)	half-life ($t_{1/2}$, in second)	rate constant (k, s^{-1})	ln k	number of water molecules	ln (no. of water molecules)
75	1.8×10^2	3.8×10^{-3}	−5.6	3.8×10^2	5.9
53	6.0×10^2	1.1×10^{-3}	−6.8	2.2×10^2	5.4
33	4.5×10^3	1.5×10^{-4}	−8.8	1.3×10^2	4.8
11[b]	1.1×10^4	6.3×10^{-5}	−9.7	1.1×10^2	4.6

[a] $t_{1/2}$ is estimated based on the time required to reached half of the A_{450} upon bleaching. Deconvoluting the FTIR spectrum of the sample equilibrated to 11% RH was not as successful as other spectra. [b] Number of water molecules estimated for that hydration level was based on the assumption that its $A_{3200cm^{-1}}$ would be between that of 33% RH and dry nitrogen. (See the Experimental Section for this linearization approximation.)

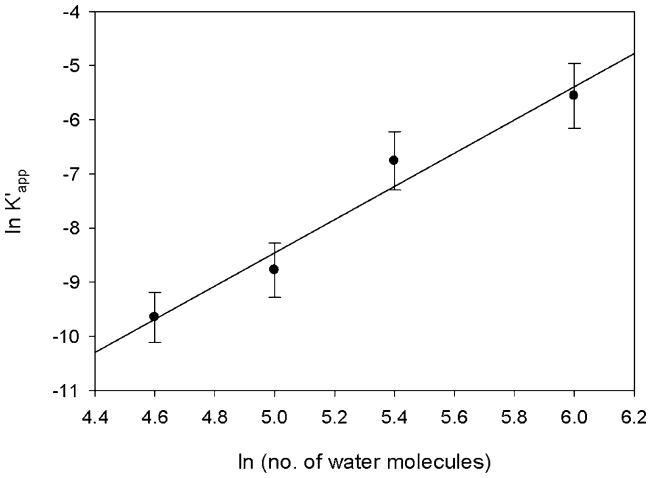

Figure 7. Linear plot of the apparent rate constant (k'_{app}) against the number of water molecules left, calculated using the FTIR water absorbance of the deconvoluted peak at 3200 cm^{-1}. Extrapolation of the plot yielded a y intercept of ln k = −23, suggesting that when there is virtually no water left, the decay rate would become infinitely slow (see text for discussion).

water exist in equilibrium and function as a reactant in the decay reaction. The observed rate of adduct decay is a first-order reaction in adduct concentration.[21] Our result indicated that the observed rate constant is in fact pseudo-first-order because the rate depends linearly on the concentration of the strongly bound water as well as the adduct.

$$\text{decay rate} = k[\text{strongly bound water}][\text{adduct}] \quad (3)$$

Assuming that the concentration of the strongly bound water does not change appreciably during the reaction the decay rate can be rewritten as

$$\text{rate} = k'_{app}[\text{adduct}] \quad (4)$$

where k'_{app} is the apparent pseudo-first-order rate constant.

$$k'_{app} = k[\text{strongly bound water}] \quad (5)$$

The logarithmic plot used therefore

$$\ln k'_{app} = \ln k + \ln[\text{strongly bound water}] \quad (6)$$

Therefore, a plot of ln k'_{app} versus ln[strongly bound water] should be linear, as observed. The number of remaining water molecules per protein molecule suggests that those water molecules may form a water cluster composed of doubly and triply bound water molecules in equilibrium in (or near) the FMN binding pocket, acting as a proton acceptor from N(5) of the isoalloxazine ring, which is the generally accepted mechanism for destabilization of the adduct's C(4)-cysteine sulfur bond.[21,48] This destabilization of the adduct results in a protonated water cluster and a thiolate. The mechanism is completed by the protonation of the thiolate back to thiol, and the water cluster returns to its original state (Figure 8).

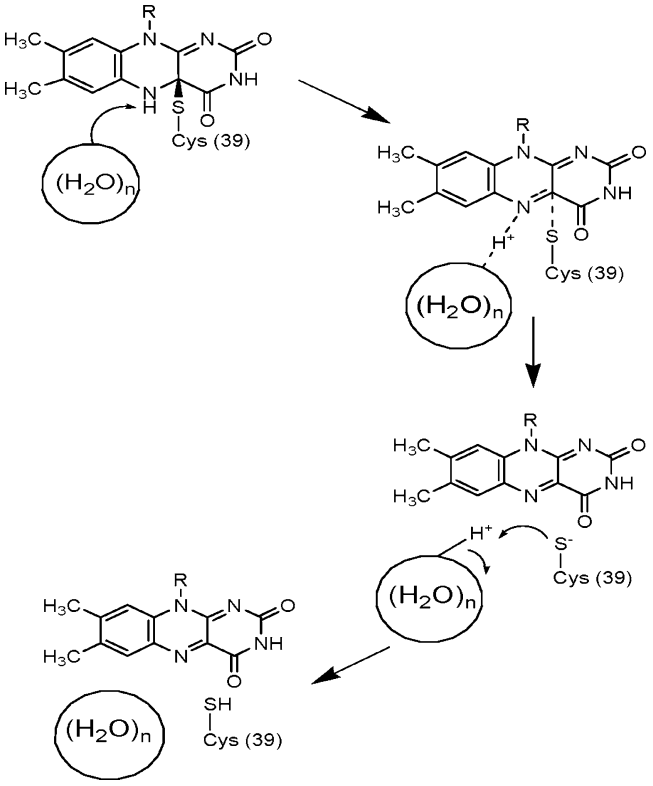

Figure 8. Adduct decay scheme and proposed mechanism for LOV2. $(H_2O)_n$ represents a possible cluster that serves as a transient proton acceptor during the decay.

The bound water concentration in the nitrogen-dried sample could be taken as an estimate of the minimal number of strongly bound water molecules/protein molecule that still allows decay of the adduct (albeit very slowly). From the data of Figure 6 and the experimental limitations described below, the number is on the order of 20−80 waters/FMN. This is only a rough approximation because the actual extinction coefficient of strongly hydrogen bonded water is not known (we used the free water coefficient), and the sample undoubtedly contains a fraction of protein molecules devoid of FMN. This chromophore loss is an unwanted consequence of the purification procedure and typically ranges between 20 and 50% of the sample depending on the conditions and age of the samples. This would decrease the value of chromophore absorption but not the concentration of strongly bound water to the chromophore-depleted apoprotein, resulting in an overestimate of the water molecules per active chromoprotein present per FMN. Strikingly the kinetics depends linearly on the bound water content, indicating that it depends on the size

dx.doi.org/10.1021/jp304934t | J. Phys. Chem. B 2012, 116, 10609−10616

of the water cluster. Extrapolation of Figure 6 to the *y* intercept (zero bound water) yields a nearly zero rate constant for adduct decay, suggesting that the back reaction would be fully blocked upon removal of the strongly bound water.

The concept of a water cluster acting as a proton relay network is not new either in the LOV domain field, as previously discussed, or in other systems, where proton-transfer mechanisms are invoked. It has been clearly demonstrated that a cluster of five or more water molecules functions as the proton release structure in bacteriorhodopsin.[49] These water clusters, containing a network of hydrogen bonds, are expected to show a semicontinuum absorption in the infrared in the 1500 to 2500 cm^{-1} region.[50]

The behavior of our films is consistent with this model. However, we cannot distinguish a model in which water is the terminal proton acceptor from one in which the water cluster relays the proton to a remote protein residue that acts as the catalytic base. One could argue that 20−80 water molecules are required to maintain protein structural integrity rather than acting as a reaction substrate or a catalyst. The consistent linear dependence of the reaction rate on bound water concentration strongly suggests that bound water acts as a substrate in the decay reaction. Extrapolation of our data to zero-bound water yields a practically infinitely large half life (on the order of 10^{10} seconds), indicating that reaction is fully blocked when the cluster is removed. It should be noted here that the crystal structures, while showing the conserved immobile structural water molecules, cannot detect the mobile water molecules from the unstructured water cluster. This is discussed at length for the bacteriorhodopsin case in the Gerwert's group publications.[49,51]

IV. CONCLUSIONS

In summary, the data show that lower hydration level slows down the adduct decay kinetics, in agreement with previous published observations,[30,31] but that kinetic control is affected by the subpopulation of strongly hydrogen-bonded structural waters. We suggest that a buried water cluster of strongly hydrogen-bonded water near the chromophore may serve as the primary proton acceptor in the proton transfer reaction or as a bridge between the flavin and a remote base in the oat phot1 LOV2 adduct decay mechanism. Previous work on the effect of dehydration on photocycle kinetics attributed the restriction to vibrational freedom as the mechanism of adduct stabilization.[31] It is possible that at the higher levels of hydration used in that work this could be a contributing factor. However, at the lower levels of hydration reached in this work, the data strongly favor the role of strongly bound water as a reactant in the decay reaction.

AUTHOR INFORMATION

Corresponding Author

*Tel: (831) 459-4294. Fax: (831) 459- 2935. E-mail: bogomol@ucsc.edu.

Notes

The authors declare no competing financial interest.

ACKNOWLEDGMENTS

This research was supported by NSF Grant MCB-0843662 (R.A.B.). We thank Dr. James W. Lewis for his assistance in designing Figure 1

ABBREVIATIONS:

FMN, flavin mononucleotide; LOV, light, oxygen, voltage; PAS, Per-Arnt-Sim; STAS, sulfate transporter anti-sigma factor

REFERENCES

(1) Briggs, W.; Beck, C.; Cashmore, A.; Christie, J.; Hughes, J.; Jarillo, J.; Kagawa, T.; Kanegae, H.; Liscum, E.; Nagatani, A.; Okada, K.; Salomon, M.; Rudiger, W.; Sakai, T.; Takano, M.; Wada, M.; Watson, J. *Plant Cell* **2001**, *13*, 993.

(2) Christie, J. M.; Reymond, P.; Powell, G. K.; Bernasconi, P.; Raibekas, A. A.; Liscum, E.; Briggs, W. R. *Science* **1998**, *282*, 1698.

(3) Christie, J. M.; Salomon, M.; Nozue, K.; Wada, M.; Briggs, W. R. *Proc. Natl. Acad. Sci. U. S. A.* **1999**, *96*, 8779.

(4) Huala, E.; Oeller, P. W.; Liscum, E.; Han, I. S.; Larsen, E.; Briggs, W. R. *Science* **1997**, *278*, 2120.

(5) Jarillo, J.; Gabrys, H.; Capel, J.; Alonso, J.; Ecker, J.; Cashmore, A. *Nature* **2001**, *410*, 952.

(6) Kagawa, T.; Sakai, T.; Suetsugu, N.; Oikawa, K.; Ishiguro, S.; Kato, T.; Tabata, S.; Okada, K.; Wada, M. *Science* **2001**, *291*, 2138.

(7) Kinoshita, T.; Doi, M.; Suetsugu, N.; Kagawa, T.; Wada, M.; Shimazaki, K. *Nature* **2001**, *414*, 656.

(8) Huang, K.; Merkle, T.; Beck, C. *Physiol. Plant.* **2002**, *115*, 613.

(9) Taylor, B. L.; Zhulin, I. B. *Microbiol. Mol. Biol. Rev.* **1999**, *63*, 479.

(10) Takahashi, F.; Yamagata, D.; Ishikawa, M.; Fukamatsu, Y.; Ogura, Y.; Kasahara, M.; Kiyosue, T.; Kikuyama, M.; Wada, M.; Kataoka, H. *Proc. Natl. Acad. Sci. U. S. A.* **2007**, *104*, 19625.

(11) Crosson, S.; Rajagopal, S.; Moffat, K. *Biochemistry* **2003**, *42*, 2.

(12) Caetano-anolles, G.; Cristestes, D. K.; Bauer, W. D. *J. Bacteriol.* **1988**, *170*, 3164.

(13) Purcell, E. B.; Siegal-Gaskins, D.; Rawling, D. C.; Fiebig, A.; Crosson, S. *Proc. Natl. Acad. Sci. U. S. A.* **2007**, *104*, 18241.

(14) Swartz, T. E.; Tseng, T. S.; Frederickson, M. A.; Paris, G.; Comerci, D. J.; Rajashekara, G.; Kim, J. G.; Mudgett, M. B.; Splitter, G. A.; Ugalde, R. A.; Goldbaum, F. A.; Briggs, W. R.; Bogomolni, R. A. *Science* **2007**, *317*, 1090.

(15) Losi, A.; Polverini, E.; Quest, B.; Gartner, W. *Biophys. J.* **2002**, *82*, 2627.

(16) Sawa, M.; Nusinow, D. A.; Kay, S. A.; Imaizumi, T. *Science* **2007**, *318*, 261.

(17) Song, Y. H.; Smith, R. W.; To, B. J.; Millar, A. J.; Imaizumi, T. *Science* **2012**, *336*, 1045.

(18) Hunt, S. M.; Thompson, S.; Elvin, M.; Heintzen, C. *Proc. Natl. Acad. Sci. U. S. A.* **2010**, *107*, 16709.

(19) Kottke, T.; Heberle, J.; Hehn, D.; Dick, B.; Hegemann, P. *Biophys. J.* **2002**, *84*, 1192.

(20) Corchnoy, S.; Swartz, T.; Lewis, J.; Szundi, I.; Briggs, W.; Bogomolni, R. *J. Biol. Chem.* **2003**, *278*, 724.

(21) Swartz, T.; Corchnoy, S.; Christie, J.; Lewis, J.; Szundi, I.; Briggs, W.; Bogomolni, R. *J. Biol. Chem.* **2001**, *276*, 36493.

(22) Losi, A.; Quest, B.; Gartner, W. *Photochem. Photobiol. Sci.* **2003**, *2*, 759.

(23) Cao, Z.; Buttani, V.; Losi, A.; Gartner, W. *Biophys. J.* **2008**, *94*, 897.

(24) Alexandre, M. T. A.; Domratcheva, T.; Bonetti, C.; van Wilderen, L. J. G. W.; van Grondelle, R.; Groot, M.-L.; Hellingwerf, K. J.; Kennis, J. T. M. *Biophys. J.* **2009**, *97*, 227.

(25) Alexandre, M.; Arents, J.; Van Grondelle, R.; Hellingwerf, K.; Kennis, J. *Biochemistry* **2007**, *46*, 3129.

(26) Crosson, S.; Moffat, K. *Proc. Natl. Acad. Sci. U. S. A.* **2001**, *98*, 2995.

(27) Fedorov, R.; Schlichting, I.; Hartmann, E.; Domratcheva, T.; Fuhrmann, M.; Hegemann, P. *Biophys. J.* **2003**, *84*, 2474.

(28) Zoltowski, B. D.; Vaccaro, B.; Crane, B. R. *Nat. Chem. Biol.* **2009**, *5*, 827.

(29) Iwata, T.; Nozaki, D.; Tokutomi, S.; Kagawa, T.; Wada, M.; Kandori, H. *Biochemistry* **2003**, *42*, 8183.

(30) Bogomolni, R. A., Swartz, T. E., Briggs, W. R. *Proceedings of the 58th Yamada Conference*; Springer: Okazaki, Japan, 2005; p 147.

(31) Iwata, T.; Yamamoto, A.; Tokutomi, S.; Kandori, H. *Biochemistry* **2007**, *46*, 7016.
(32) Zoltowski, B. D.; Nash, A. I.; Gardner, K. H. *Biochemistry* **2011**, *50*, 8771.
(33) Nozaki, D.; Iwata, T.; Ishikawa, T.; Todo, T.; Tokutomi, S.; Kandori, H. *Biochemistry* **2004**, *43*, 8373.
(34) Lasagabaster, A.; Abad, M. J.; Barral, L.; Ares, A. *Eur. Polym. J.* **2006**, *42*, 3121.
(35) Roge, B., Aroulmoji, V., Mathlouthi, M. *Water Properties of Food, Pharmaceutical, and Biological Materials*; Taylor & Francis Group: Boca Raton, FL, 2006; p 583.
(36) Hoad, S. P.; Grace, J.; Jeffree, C. E. *J. Exp. Bot.* **1997**, *48*, 1969.
(37) Varo, G.; Lanyi, J. K. *Biophys. J.* **1991**, *59*, 313.
(38) Young, J. F. *J. Appl. Chem.* **1967**, *17*, 241.
(39) Laporta, M.; Pegoraro, M.; Zanderighi, L. *Phys. Chem. Chem. Phys.* **1999**, *1*, 4619.
(40) Cotugno, S.; Larobina, D.; Mensitieri, G.; Musto, P.; Ragosta, G. *Polymer* **2001**, *42*, 6431.
(41) Thouvenin, M.; Linossier, I.; Sire, O.; Peron, J. J.; Vallee-Rehel, K. *Macromolecules* **2002**, *35*, 489.
(42) Salomon, M.; Christie, J.; Knieb, E.; Lempert, U.; Briggs, W. *Biochemistry* **2000**, *39*, 9401.
(43) Barbetta, A.; Edgell, W. *Appl. Spectrosc.* **1978**, *32*, 93.
(44) Chaplin, M. Water Structure and Science. www.lsbu.ac.uk/water/vibrat.html. Accessed May 21, 2012.
(45) Cantor, C. R., Schimmel, P. R. *Biophysical Chemistry Part II: Techniques for the Study of Biological Structure and Function*; W. H. Freeman and Company: New York, 1980.
(46) Szundi, I.; Swartz, T. E.; Bogomolni, R. A. *Biophys. J.* **2001**, *80*, 469.
(47) Grdadolnik, J. *Maced. J. Chem. Chem. Eng.* **2002**, *21*, 23.
(48) Christie, J. M.; Corchnoy, S. B.; Swartz, T. E.; Hokenson, M.; Han, I. S.; Briggs, W. R.; Bogomolni, R. A. *Biochemistry* **2007**, *46*, 9310.
(49) Garczarek, F.; Gerwert, K. *Nature* **2006**, *439*, 109.
(50) Zundel, G. *Adv. Chem. Phys.* **2000**, *111*, 1.
(51) Garczarek, F.; Brown, L. S.; Lanyi, J. K.; Gerwert, K. *Proc. Natl. Acad. Sci. U. S. A.* **2005**, *102*, 3633.